Blucher Mechanical Engineering Proceedings
May 2014, vol. 1 , num. 1
www.proceedings.blucher.com.br/evento/10wccm

10th World Congress on Computational Mechanics
8-13 July 2012 • São Paulo • Brazil

VIBRATION REDUCTION BY LANDSCAPE SHAPING AT HIGH-TECH FACILITY

P. Persson[1], K. Persson[1], P. Jørstad[1], G. Sandberg[1]

[1]Division of Structural Mechanics, Lund University, Sweden (peter.persson@construction.lth.se)

Abstract. *This paper presents a numerical study on the reduction of vibrations in the ground. The influence of landscape shaping to reduce vibration levels induced by traffic is investigated by means of the finite element method with dynamic analyses. Both two-dimensional as well as three-dimensional finite element models are employed for the investigations. A harmonic point force is applied where the force is scaled to represent the frequency dependent traffic load. Finally, the vibration reduction effect is evaluated by comparing RMS-values at a number of different evaluation points. It is concluded from the analyses that the two-dimensional and three-dimensional models correlates fairly well. The performance of a hill is increased if it is preceded by a valley but when applying more valleys than hills, amplification may occur. When using continuous hills instead of a checkered pattern, the hills seem to capture and guide waves in the direction of the hill. Locally this could reduce vibrations of significant importance. Applying the constraints given within the numerical example, vibration reductions of approximately 20 % could be seen.*

Keywords: *Shaped landscape, Vibration reduction, Wave propagation, Soil dynamics, Finite element method.*

1. INTRODUCTION

1.1. Problem formulation

In this paper, vibration reduction at a high-tech facility will serve as a numerical example. The high-tech facility is called MAX IV, see Figure 1 for an architectural sketch. A new storage ring is needed to improve research possibilities. The research fields are e.g. material science and medicine. The storage ring is controlled by a large number of magnets that are distributed along the ring. Since the quality of the measurements is dependent on the vibration levels of the magnets, a very strict requirement regarding the vibration levels is specified. The strict requirement is especially put on the mean vertical vibration level that must be less than 26 nm during one second in the frequency span 5-100 Hz.

The goal is to investigate the reduction of traffic-induced vibrations by applying different shapes to an initially flat landscape. The aim is to evaluate the influence of landscape shaping to minimize the vibration levels in the MAX IV facility.

From previous work it has been concluded that the parameters of the soil have a large influence on the vibration levels in the storage ring tunnel, therefore the influence of landscape shaping was investigated. This was done by establishing a finite element model that can predict the influence of the vibration levels, by landscape shaping, with high accuracy. The vibrations were analysed by means of the finite element method with dynamic analysis. The investigation was focused on the vertical vibration amplitudes. The geometric and mechanical constraints, determined by the MAX IV project, were applied. Two-dimensional parametric studies as well as three-dimensional analysis for were performed.

1.2. Previous work

The MAX IV facility and its surrounding landscape were analysed by the finite element method in a report, [10]. It was concluded from the analyses that the material parameters of the soil have a significant influence on the vibration levels in the facility and more reliable material parameters are needed for the finite element analysis to achieve more reliable results. A comparison between measurements at the construction site of the facility and results from the finite element model were carried out in, [11]. It was concluded that the measurements and the calculations correlated fairly well. The finite element model was also improved in the sense of accuracy and computational cost. In, [12], the influence of using trenches to reduce vibration levels in the facility, induced by traffic, was investigated. A frequency dependent factor was applied to scale the unit harmonic load to represent the traffic load on the nearby highway. It was concluded from the analysis that modifications of the soil, in the sense of trenches, could reduce the vibration levels of more than 50 % of the RMS-value of the vertical displacements. In the previous work it was also concluded that the frequencies over 20 Hz in the traffic load have negligible influence on the displacements in the facility.

1.3. Literature review

A solution for two-dimensional scattering and diffraction of plane P, SV and SH waves by canyons of arbitrary shape in an elastic half space is presented by Lee and Wu in [6, 7]. The displacements are computed numerically with the method of weighted residuals (moment method). It was concluded that ground amplifications are frequency dependent and also depends on the orientation of the incident wave. Lee and Wu concluded that the shape of the canyon had an effect on the displacement amplitudes at the surface of the canyon and the nearby half space [7]. They also state that their presented method also may be extended to consider alluvial valleys. Diffraction of plane harmonic waves by three-dimensional surface irregularities was investigated, by Mossessian and Dravinski [8], with use of the indirect boundary integral method. The irregular shapes are arbitrary and embedded in the half-space. They found that it is important to use three-dimensional models when investigating scattering

of elastic waves by surface topographies of arbitrary shape. Reinoso, Wrobel and Power [13] investigated three-dimensional scattering of seismic waves from irregular topographies by the direct boundary element method. The irregular shapes were both mountains as well as valleys. They found that an irregularity, such as a mountain, affecting the amplification of the motion by its geometry. They also found that vertical walls will generate higher amplifications than a mountain with a smooth slope. Sánchez-Sesma and Campillo [15] investigated the topographical effects of waves in an elastic half-space using indirect BEM. They found that topography may have significant influence on both amplification and de-amplification at and nearby the irregular shape. Zhou and Chen [16] investigated the influence of topography on Rayleigh waves, excited by an explosive source near the surface. They compared the energy of the wave and the frequency, before and after passing the topography, in order to evaluate the influence of the steepness of the topography. They found a reduction of the energy of the wave and a loss of high frequency content. These effects were more obvious with a steeper topography.

In this paper the finite element method is employed to investigate the influence of irregularities in the ground on surface vibrations, an approach not taken by earlier studies. By using the finite element method different materials in the ground may be considered. In this paper also the frequency dependent traffic load is taken into account. The objective of this paper differs from the papers mentioned above. This paper is more focused on the possibility to reduce incident waves with irregularities, e.g. a shaped landscape.

1.4. Landscape shaping

At large construction sites, large amounts of soil will be excavated in order to smooth the surface. This is necessary since the surface needs to be horizontal before the construction of the facility may start. The large amount of soil often needs to be transported away from the construction site, which may be costly for the project. These masses of soil may instead be useful at the construction site. The masses could be used to construct a shaped landscape with hills and valleys. The shaped landscape could contribute to reduce external vibrations at the facility but there are uncertainties regarding the potential of the reduction of traffic-induced vibrations. The vibration sources may be traffic and trains. The excavation of soil and the construction of hills open a possibility to also construct valleys at the site. The architects in the MAX IV project have developed a geometry for a shaped landscape of the surroundings of MAX IV facility, the idea was induced by the Division of Structural Mechanics at Lund University. The shaped landscape is an aesthetically desirable solution. In Figure 1 a proposal for the MAX IV facility with shaped landscape by the architect bureaus Fojab and Snøhetta is shown. Various constraints are applied for the shaped landscape. A material constraint is that the present clay till will be used for the hills. A geotechnical constraint is the slope angle of the hills and valleys which is determined to be 30 degrees. An architectural constraint is that the hills and valleys should have a rounded shape, i.e. the formations will have a smooth and natural design.

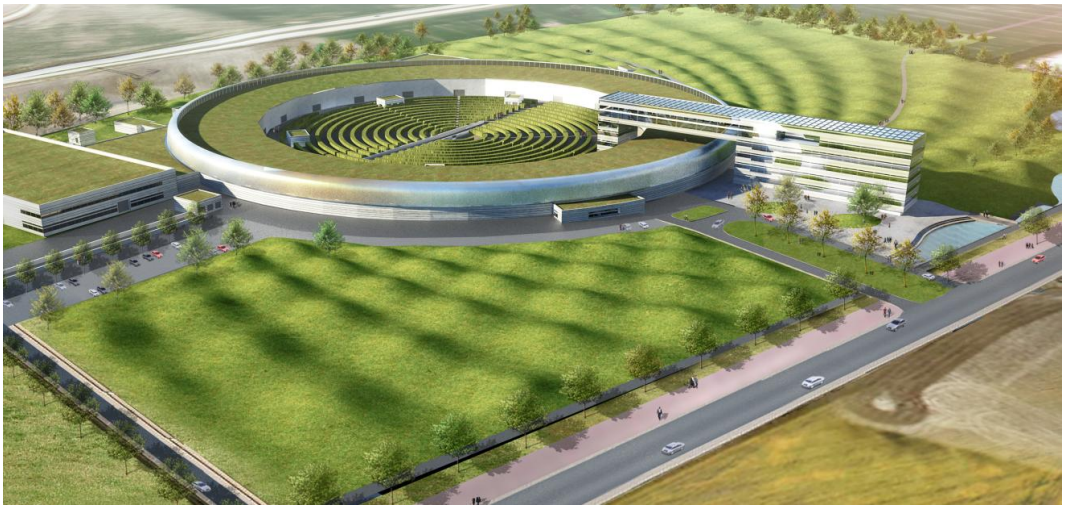

Figure 1. Shaped landscape at MAX IV facility, by the architect bureaus Fojab and Snøhetta.

Figure 2. Aerial photograph at construction site of MAX IX, by photographer Perry Nordeng, March 2012.

2. GOVERNING THEORY

2.1. Structural dynamics

For further reading about the finite element method and structural dynamics as well as for reference, see e.g. [2-4, 17].

Partial differential equations are often used to describe various physical problems and are often too complicated to be solved in an analytical manner. Therefore, numerical methods may be required. Such a method is the finite element method, FEM, that solves arbitrary boundary valued differential equations with arbitrary geometry and material. The equation of motion of a body assuming small deformations may be described by the differential equation

$$\tilde{\boldsymbol{\nabla}}^T \boldsymbol{\sigma} + \boldsymbol{b} = \rho \frac{\partial^2 \boldsymbol{u}}{\partial t^2} \tag{1}$$

where $\tilde{\boldsymbol{\nabla}}$ is a differential operator matrix, $\boldsymbol{\sigma}$ the stress vector, $\boldsymbol{b}$ the body force vector, ρ the mass density, $\boldsymbol{u}$ the displacement vector and t is the time. Velocity dependent damping forces are not introduced in the derivations. The governing finite element formulation of the dynamic problem may be written as

$$\boldsymbol{M}\ddot{\boldsymbol{u}} + \boldsymbol{K}\boldsymbol{u} = \boldsymbol{p} \tag{2}$$

where $\boldsymbol{K}$ is the stiffness matrix, $\boldsymbol{M}$ the mass matrix, $\boldsymbol{p}$ the load vector and $\boldsymbol{u}$ the displacement vector. By not introducing velocity dependent damping forces, the damping matrix is not considered.

With harmonic loading a steady-state vibration will occur. The load and the corresponding displacements may be expressed as complex harmonic functions

$$\boldsymbol{p} = \hat{\boldsymbol{p}} e^{i\omega t} \tag{3}$$

$$\boldsymbol{u} = \hat{\boldsymbol{u}} e^{i\omega t}$$

where $\hat{\boldsymbol{p}}$ and $\hat{\boldsymbol{u}}$ denotes the complex load and displacement amplitudes, i is the complex number, is the angular frequency and t the time. Inserting Eq. 2 in Eq. 1, Eq. 1 may be written as the equation of motion in the frequency domain

$$\boldsymbol{D}(\omega)\hat{\boldsymbol{u}} = \hat{\boldsymbol{p}} \tag{4}$$

where $\boldsymbol{D}(\omega)$ is the frequency dependent dynamic stiffness matrix and is expressed as

$$\boldsymbol{D}(\omega) = -\omega^2 \boldsymbol{M} + \boldsymbol{K}. \tag{5}$$

To introduce damping in the system the loss factor is used. The loss factor is defined as

$$\eta = \frac{1}{2\pi} \frac{E_D}{E_{So}} \tag{6}$$

where in steady-state, the energy dissipated in viscous damping in one cycle of harmonic vibration is denoted E_D and the strain energy is denoted E_{So}. With use of the loss factor, the damping matrix is the imaginary part of the stiffness matrix, known as the structural damping matrix. The dynamic stiffness matrix may now be written as

$$\boldsymbol{D}(\omega) = -\omega^2 \boldsymbol{M} + (1 + i\eta)\boldsymbol{K}. \tag{7}$$

The Root Mean Square value, RMS-value, is used as a measure of the magnitude of a vibration. The RMS-value of displacements from a steady-state analysis is determined as

$$u_{RMS} = \sqrt{\frac{1}{n}(u_1^2 + u_2^2 + \cdots + u_n^2)} \tag{8}$$

where u_{RMS} is the RMS-value of displacements, u_i is the magnitude of the frequency dependent displacement and *n* is the number of frequencies in the interval.

2.2. Wave propagation

For further reading about the wave propagation and for reference, see e.g. [1, 5, 14].

For human induced ground vibrations, stresses are usually at such a level that an assumption of linear elasticity is applicable. Damping generally plays an important role in terms of the dynamic response in soils and is therefore often considered in the linear elastic material model, which makes it a visco-elastic material model.

Soil is not a homogenous material, e.g. due to the granularity of soil. However, for wave propagation, local variations do not have a large influence. If the local variations in the soil are small compared to the wave lengths, then soil may be modelled as a homogenous material.

3. MATERIAL PROPERTIES

In the numerical example, MAX IV, the area between the highway and the facility consists of 14 m layer of soil, Low Baltic clay till, and bedrock consisting of shale. Since the materials are exposed to loads with low magnitude and the wave lengths are long compare to local variations, the pre-consolidated clay till as well as the shale were modelled as linear elastic isotropic materials. The material parameters, determined by geotechnical consultants in the MAX IV project, is shown in Table 1. The loss factor includes material damping and other attenuation effects, such as varying topology of the soil as well as the bedrock.

Table 1. Material properties for the clay till and for the shale.

Property	Clay till	Shale
Depth	14 m	-
Young's modulus	476 MPa	8809 MPa
Density	2125 kg/m^3	2600 kg/m^3
Poisson's ratio	0.48	0.40
Loss factor	0.14	0.10

4. TRAFFIC LOAD

Vibration measurements have been performed at the construction site of MAX IV by consultants in the MAX IV project. To evaluate the traffic load from the nearby highway, green-field in-situ measurements were performed. The velocities were measured at a location 100 m from the highway, the same distance as between the highway and the facility. Vertical displacements were evaluated for 1/3-octave bandwidths. In Table 2 the vertical displacements are shown, [9].

Table 2. Vertical displacements versus frequency for 1/3-octave bandwidths.

Frequency [Hz]	Vertical displacement [nm]
5	28.8
6.3	46.4
8	38.0
10	37.0
12.5	15.0
16	7.30
20	1.50

The evaluated displacements may be used, together with the calculated displacements from a frequency response function, to determine a traffic load according to Eq. 9.

$$p_{traffic\ load} = \frac{U_{measurements,green-field}}{U_{FRF,green-field}} p_{FRF}. \quad (9)$$

In the frequency response function, FRF, a unit load is applied, i.e. p_{FRF} will be equal to 1 for every frequency. The traffic load is assumed to vary linearly between the 1/3-octave bands.

5. FE-MODEL AND NUMERICAL STUDY

The numerical analyses were performed by means of the finite element method with dynamic analysis. FE-model, results and discussion of the results for two-dimensional and three-dimensional parametric studies are presented respectively.

The finite element software *HyperWorks* was used for the finite element analyses. For solution of large FE models where high computational performance is needed the computational resources for computational science at Lund University, LUNARC, were used. The finite element programs were run on a high performance cluster, *Platon*, belonging to LUNARC.

5.2. Two-dimensional study

A state of plane strain was assumed for the two-dimensional analyses. Parametric studies using steady-state analyses were performed for a frequency span of 5-20 Hz in steps of 0.5 Hz.

An initial study was performed to determine the size needed for the finite element model to avoid reflections from the boundaries. To avoid reflection waves form the boundary a model with dimensions 560x200 m^2 was used in the analyses. The elements used were 4-node elements applying plane strain conditions with linear approximation. The element size was set to 2x2 m^2 to accurately describe the arc-shaped hills and valleys. The model ended up at 29 960 elements with a total of 120 714 dofs.

The load is applied as a harmonic concentrated load in a node in the middle of the top surface of the model. The load is scaled to represent the traffic load on the nearby highway,

see Eq. 9. The finite element model had no applied boundary displacements, implying net zero force condition in the steady-state solution.

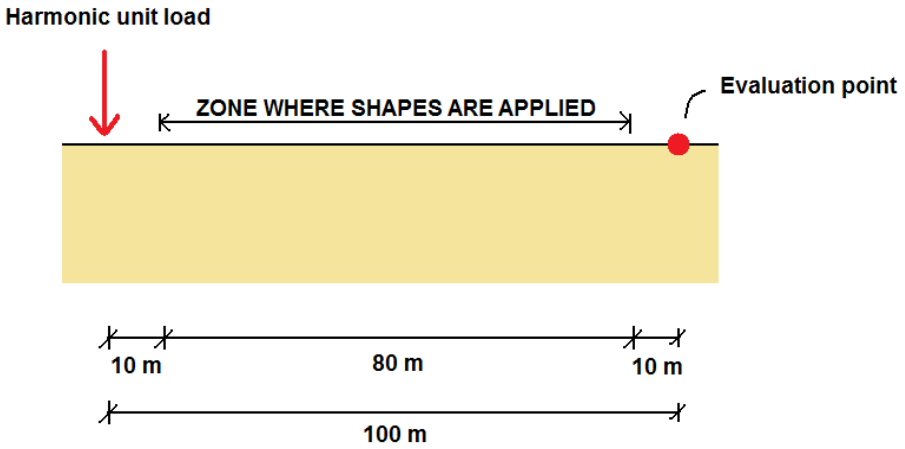

Figure 3. Location of excitation point, evaluation point and the zone where the shapes were applied.

The shapes were applied at a zone of 80 m, starting 10 m from the excitation point and ending 10 m from the evaluation point, see Figure 4. A constant curvature of the arcs that create the shapes was put as a constraint with a maximum slope of 30 degrees. A total of six different arcs were used to create the shapes. The shapes are denoted 2DShape1-2DShape6, where 2DShape1 implies 1 arc stretching over the entire distance of 80 m. In the same manner 2DShape6 has 6 arcs stretching over the distance. See Table 3 for the dimensions of the individual arcs. In Figure 4 the geometry of the individual arcs is shown.

Table 3. Width and height of the individual arcs.

Shape notation	Width, l [m]	Height, h [m]
2DShape1	80.0	10.7
2DShape2	40.0	5.36
2DShape3	26.7	3.57
2DShape4	20.0	2.89
2DShape5	16.0	2.14
2DShape6	13.3	1.79

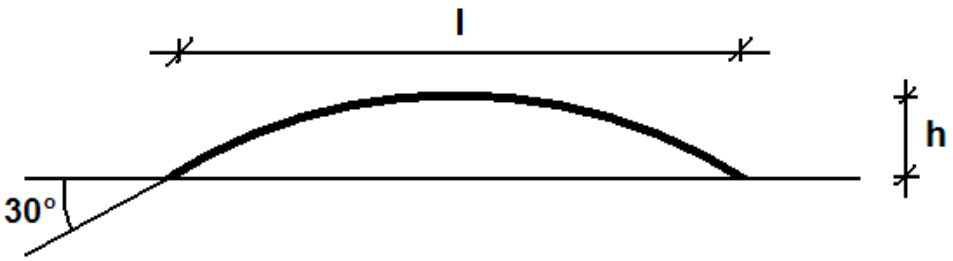

Figure 4. Geometry of the individual arcs.

In order to denote whether the shapes creates hills or valleys an extra notation was introduced according to [Z]2DShapeX[Y_Y_..._Y], where X denotes number of arcs and Y is either 1 or -1, where 1 implies a hill and -1 implies a valley and. Z denotes a global shape factor that was used to describe the geometric scale factor of the applied hills and valleys. The global shape factor could be either positive or negative.

The numerical investigation showed that several of the shapes generated a significant reduction of the vertical displacements at the evaluation point. Moreover, shapes that generated a net addition of mass or no change in mass of the model, always gave a reduction of the displacements. The shapes that generated the largest reduction in vertical displacements were 2DShape2 and 2DShape3 with altering hills and valleys. It was noticed in all configurations with an even number of arcs that, a hill preceded by a valley gave an increased reduction, which implied that the positive effect of a hill is increased when it is preceded by a valley rather than the abrupt inclination from a flat terrain. For 2DShape4, 2DShape5 and 2DShape6 the configuration that generated the highest reduction was when only hills were applied. For these configurations (2DShape4-2DShape6), a negative change in total soil volume always led to an amplification of the displacements. For the shape 2DShape1 significant reduction for negative global shape factor of large magnitude occurred, whereas for a global shape factor of -0.25 it gave amplification. 2DShape5 performed poorly with a negative global shape factor with altering hills and valleys. For 2DShape4 and 2DShape6 the global shape factor, not depending on if it is positive or negative, had the same influence. For all positive global shape factors a reduction was found. Responses were also extracted at a point 10 m from the main evaluation point, i.e. 20 m from the shaped zone and 110 m from the excitation point, for all configurations with global shape factors of 1 and -1. This was done to verify that the responses at the main evaluation point were not a result of some local phenomenon. These responses showed the same tendencies as for the main evaluation point. For the two best performing configurations a frequency plot is shown in Figure 5. A reduction in displacements, almost throughout the whole frequency span, for both configurations is shown. With the configuration [-1]2DShape2, the maximum reduction in the RMS value of 24.7 % was obtained.

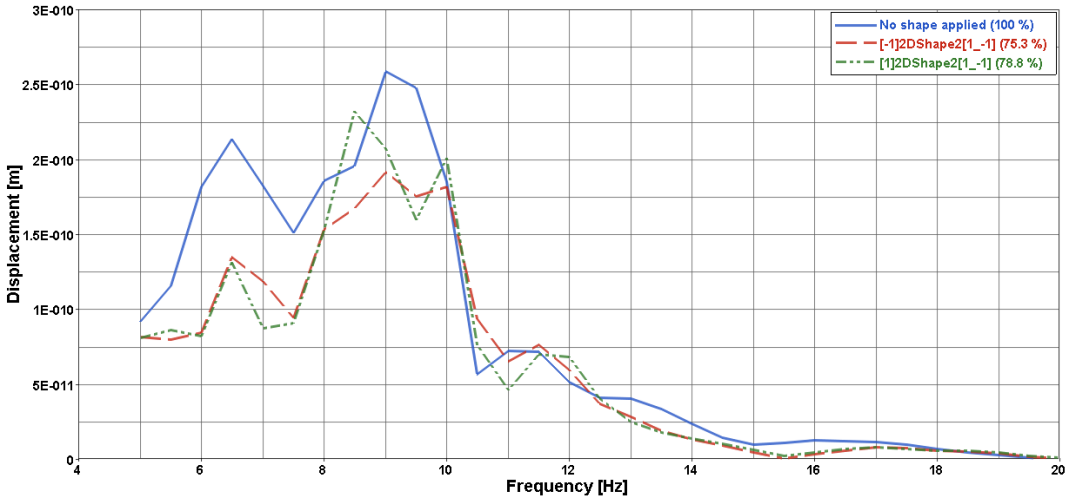

Figure 5. Plot of vertical displacements versus frequency for the two best configurations.

5.3. Three-dimensional study

Parametric studies using steady-state analyses on three-dimensional geometries were performed for the frequency span 5-20 Hz in steps of 1/3-octave bands.

The dimensions of the geometry were set to 400x400x114 m^3 where 114 m consists of 14 m soil and 100 m bedrock. The elements used were 8-node solid elements with linear approximation. The model was meshed symmetrically in the horizontal (x-y) plane. The element size was set to 2x2 m^2, in the shaped zone, to accurately describe the arc-shaped hills and valleys. This element size was used in a 120 m long zone stretching from the excitation point, followed by zones with increasing element sizes up to a length of 10 m. In the vertical direction (z-direction), elements of 2 m are used in the soil. In the bedrock, the first eight elements in the vertical direction were 4 m, then six 6 m, then four 8 m. The bedrock is significantly stiffer than the soil which will contribute to longer wavelengths, hence the increased element size compared to the elements in the soil. The element sizes fulfil requirements regarding the wave lengths. The model ended up at 518 400 elements with a total of 1 093 358 dofs. In Figure 6 the finite element mesh of a quarter of the three-dimensional model is shown.

The load was applied as a harmonic concentrated load in one node in the centre of the top surface of the model, see Figure 7. The load was scaled analogously to the two-dimensional case, according to Table 3. Due to the scattering of the propagating waves in three dimensions, the displacements were evaluated along a straight line, 100 m from the excitation point. 10 evaluation points were placed along that line with the main evaluation point in the middle corresponding to the shortest distance to the excitation point. In Figure 7 the location of the main evaluation point is shown. The finite element model had no applied boundary displacements, implying net zero force condition in the steady-state solution.

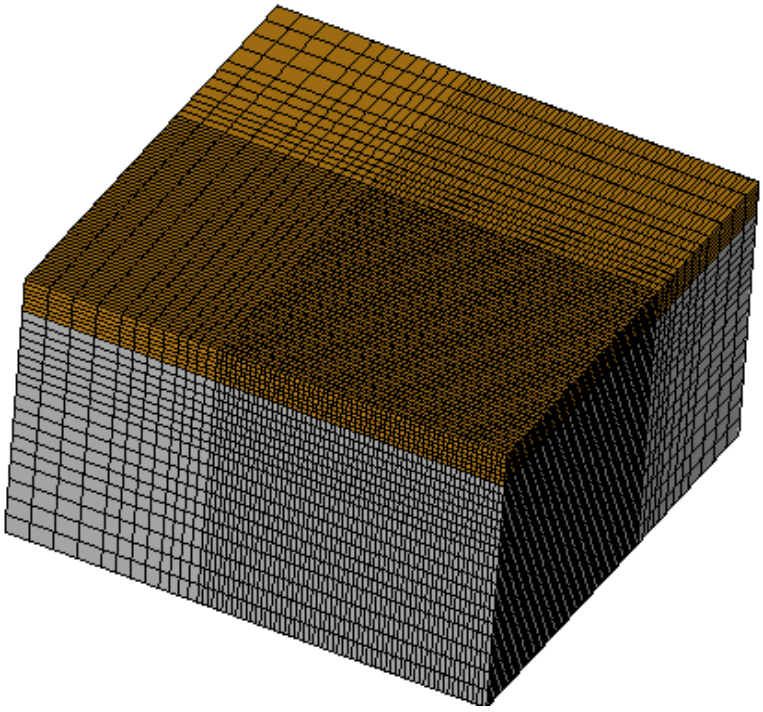

Figure 6. Finite element mesh of a quarter of the three-dimensional model.

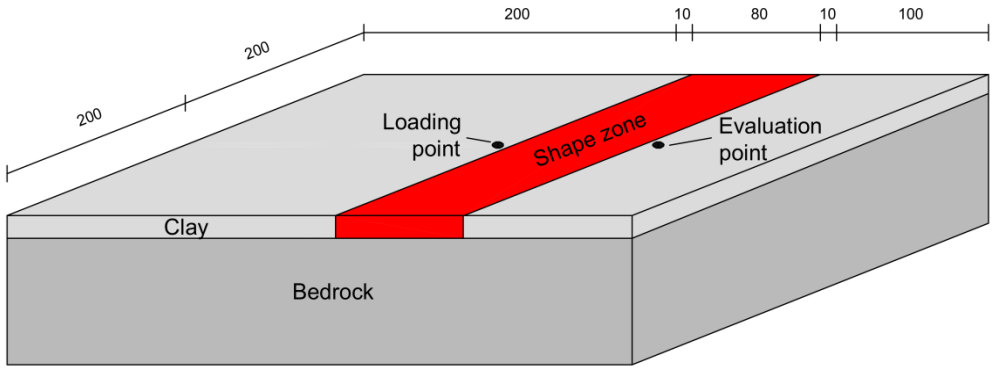

Figure 7. Location of excitation point, evaluation point and the zone where the shapes are applied.

Three various principal shape patterns were investigated. In Figure 7 the location of the shape zone is shown. The three-dimensional shapes follow the same name convention as in the two-dimensional study. The initial version of shapes applied to the three-dimensional model corresponds to the shapes applied for the two-dimensional model, i.e. the arcs in the two-dimensional model were extruded in the direction parallel to the evaluation points. In Figure 8 an example of a straight 3D shape is shown. The next version considers rotated extruded arcs. The extruded arcs are rotated 45 degrees in the horizontal plane. The difference to the previous version is that the incident surface waves will have another incident angle. In Figure 10 an example of a rotated 3D shape is shown. The third version is constructed as a checkered pattern of hills and/or valleys. This version resembles the architectural design, see Figure 1. In Figure 12 an example of a checkered 3D shape is shown. To compare with the values presented for the two-dimensional analyses with the three-dimensional, the response at the main evaluation point was used.

For the straight 3D shapes, the values of RMS vertical displacements showed that all configurations, except for the ones where only valleys were present, generated a vibration reduction. As for the two-dimensional results, 3DShape2_Straight generated the largest vibration reduction, with a maximum reduction of 24.1 % of the RMS-value of vertical displacements at the main evaluation point for the [-1]3DShape2[1_-1]_Straight configuration. Larger reductions were found in the additional evaluation points with a maximum reduction of approximately 30 % for the mentioned best performing configurations. In the visualizations of the results it was shown that a part of the wave was captured in the first hill and reflected inside the hill along the hill. This phenomenon was the reason why relatively larger reductions were found in the additional evaluation points, as the wave fronts approaching these points were guided along the hill. Ultimately, this was also the reason why hills and valleys rotated 45 degrees in the horizontal plane were investigated as an attempt of trying to capture and guide the waves to an larger extent. In Figure 9 a plot of vertical displacement versus frequency for some straight 3D shapes is shown.

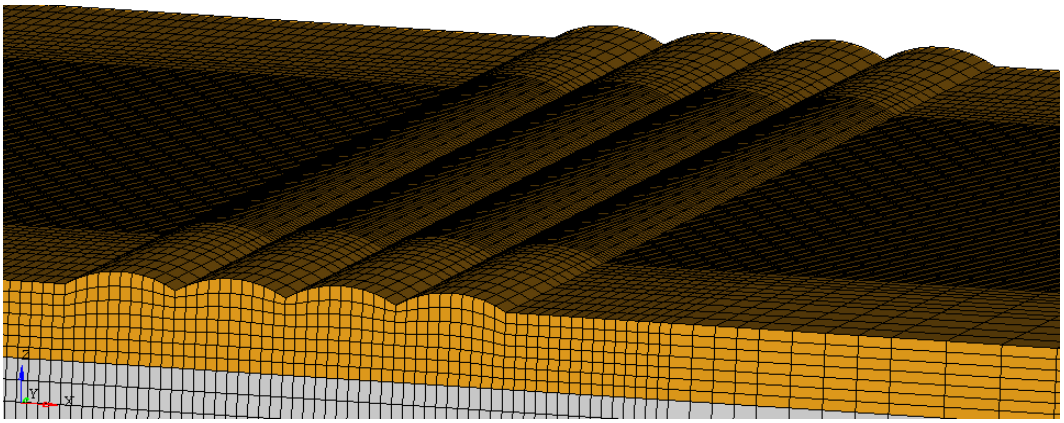

Figure 8. Example of a straight 3D shape, [1]3DShape4[1_1_1_1]_Straight.

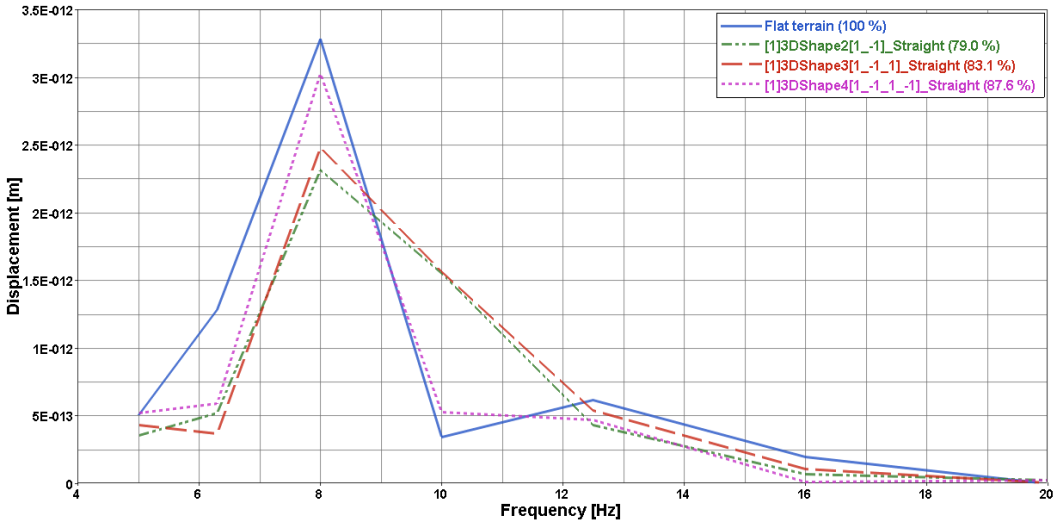

Figure 9. Plot of vertical displacement versus frequency for some straight 3D shapes.

The horizontally rotated, 45 degrees, shapes were different from the straight shapes by being non-symmetrical. This results in that the responses in the additional evaluation points vary depending on which side of the main evaluation point that was evaluated. In some configurations there was vibration reduction on one side and amplification on the opposite side. The differences in effects are however not unexpected, as the phenomenon of waves being guided by the hills has already been observed for the straight shapes. In the case of 3DShape2[1_-1]_45, a positive global shape factor generates a significantly different response than for a negative global shape factor. A negative global shape factor for the same configuration, generated vibration reduction of approximately 50 % in the majority of the evaluation points and was concluded to be best performing shape configuration. A negative shape factor of the 3DShape_45 shapes, only valleys, always generated amplification. Applying only hills generated vibration reduction in all evaluation points except for the main evaluation point of [1]3DShape4[1_1_1_1]_45 where a negligible amplification was observed. In Figure 11 a plot of vertical displacement versus frequency for some rotated 3D shapes is shown.

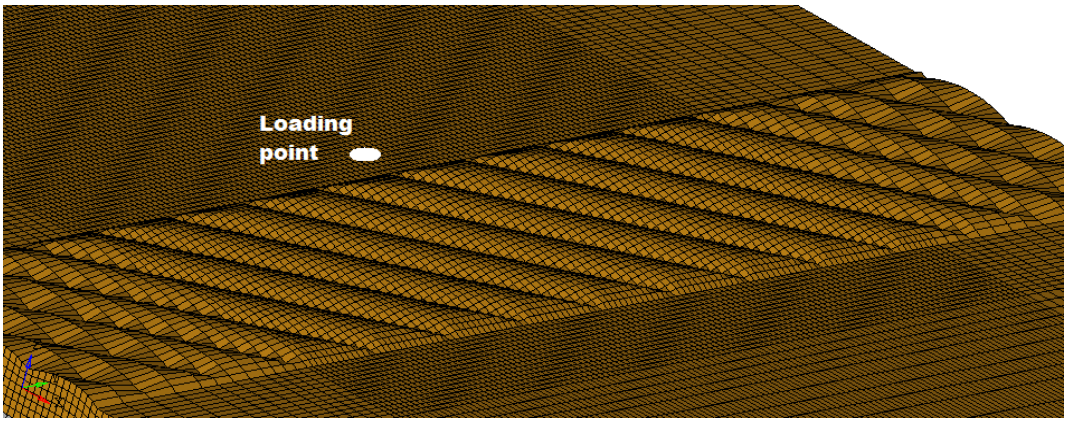

Figure 10. Example of a rotated 3D shape, [1]3DShape4[1_1_1_1]_45.

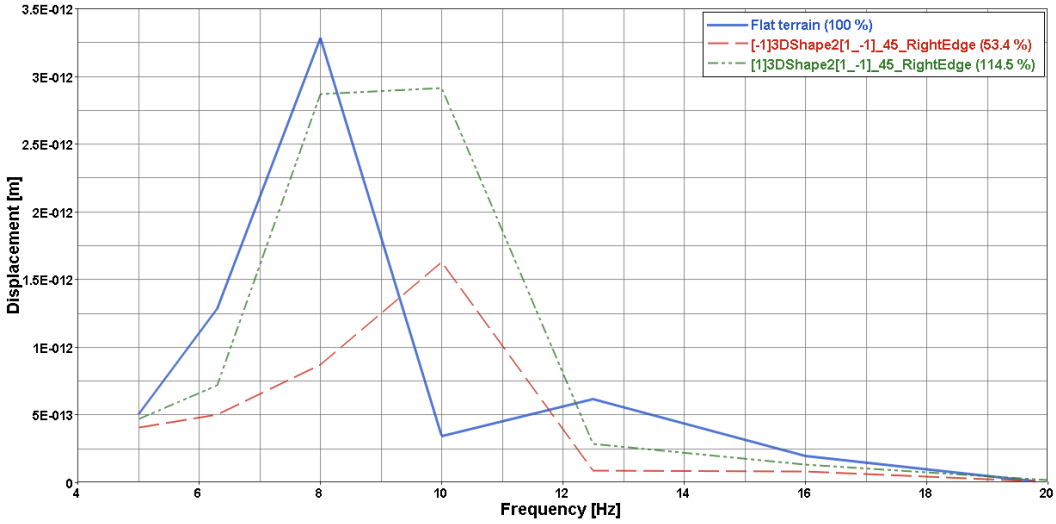

Figure 11. Plot of vertical displacement versus frequency for some rotated 3D shapes.

Checkered shapes were constructed of hills and/or valleys. Consistent with respect to the previously presented results, if only valleys are applied amplifications were found at the evaluation points. Less consistent with respect to the previously presented results, in the configurations 3DShape3[1_1_1]_Check and 3DShape4[1_1_1_1]_Check, amplification was found at the main evaluation point and the nearby additional evaluation points. If both hills and valleys were applied, all tested configurations of 3DShape4_Check generated vibration reduction in all the evaluation points. Some of the configurations, derived from the larger arcs, led to amplification in some evaluation points. From the visualizations it was evident that 3DShape4_Check with both hills and valleys created more obvious diagonals made up of hills into which the waves were captured and guided, analogously to the rotated shapes. In Figure 13 a plot of vertical displacement versus frequency for some checkered 3D shapes is shown.

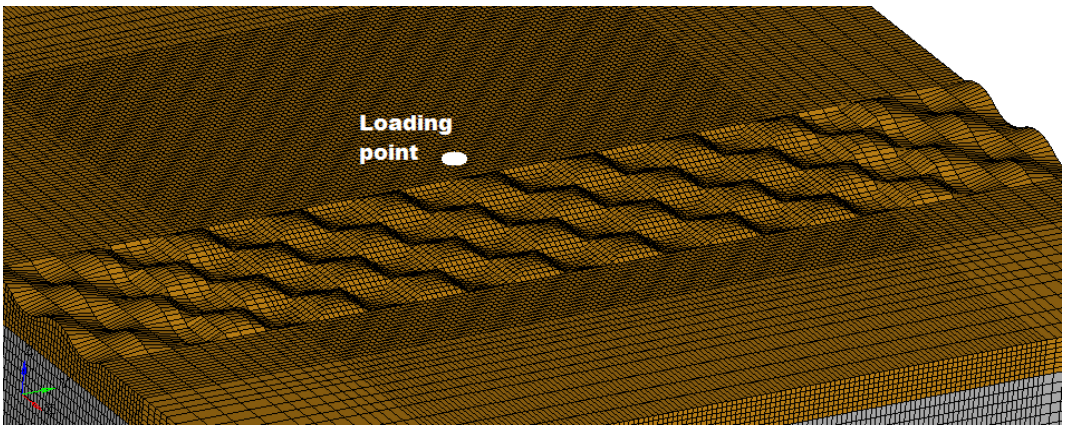

Figure 12. Example of checkered 3D shape, [1]3DShape4[1_-1_1_-1]_Check.

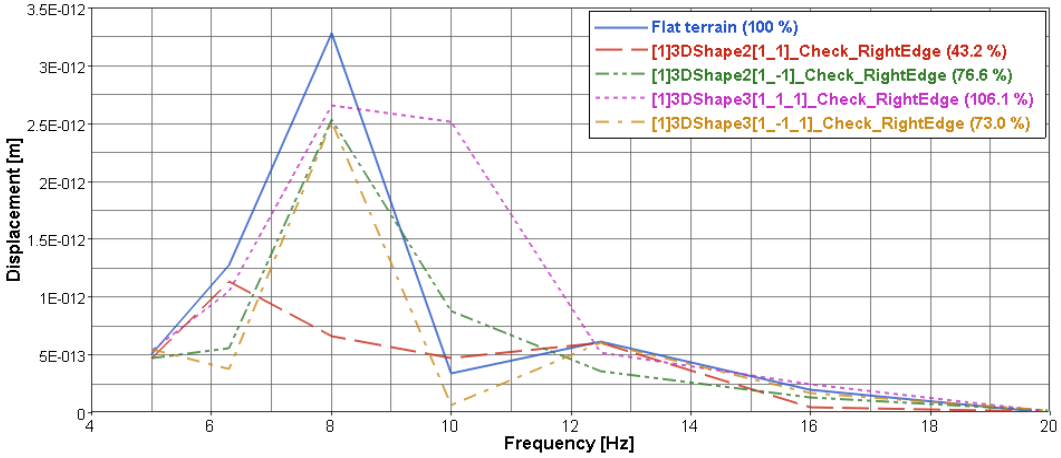

Figure 13. Plot of vertical displacement versus frequency for some checkered 3D shapes.

5.4. Discussion and comparison

An aspect of the two-dimensional plane strain analyses is the fact that the loading translated into three dimensions would correspond to a line load, not a concentrated load as in the three-dimensional analyses. A concentrated load gives a more correct modelling of the traffic load.

The three-dimensional finite element model seems to perform well in the zone where the vibrations are of interest. A peak of significant importance in the response may be missed due to the large steps in the frequency span, thus smaller steps may be needed to refine the analysis.

A fact that strengthens the conclusions drawn from the three-dimensional analyses in general is that the corresponding two-dimensional and straight three-dimensional shapes show similar results and a similar magnitude of vibration reduction.

6. CONCLUSIONS

For the two-dimensional finite element analyses, the following conclusions may be drawn:

- Applying altering hills and valleys generates vibration reduction for a positive or zero change in total volume of the soil (the latter implying an even number of hills and valleys).
- A few larger sized hills are more efficient in reducing vibrations than several smaller sized hills, stretching over the same zone.
- For smaller sized hills, the best solution is to apply hills exclusively.
- If the dimensions are sufficiently large, a smooth transition between valleys and hills increase the reduction of the hill compared to an abrupt transition between two hills.
- Generally, when applying more valleys than hills, amplification is obtained. If the dimensions of the shapes are sufficiently large, vibration reduction could is obtained.
- The two best performing shapes are altering hills and valleys with two arcs. A vibration reduction of approximately 25 % is seen for the best performing shape.

For the three-dimensional finite element analysis, the following conclusions may be drawn:

- Generally, applying only valleys generates amplification.
- Larger sized hills give larger reduction than smaller sized hills.
- A smooth transition between hills and valleys may increase the reduction of the hill compared to an abrupt transition between two hills.
- With application of straight 3D shapes, vibration reduction of approximately 20 % is obtained.
- Continuous hills seem to capture and guide waves in the direction of the hill. This effect depends on the angle of the incident wave. By rotating the hills in the horizontal plane, local vibration reductions of up to 50 % is obtained. However, hills that have direction component towards the evaluation point may also guide waves and thus generates amplification.
- A regular checkered pattern of hills and valleys behaves in the same manner as continuous hills. Waves follow the paths of neighbouring hills, depending on the angle of the path and the direction of the wave. Applying only valleys generates amplification. Whereas applying only hills may create a straight path between the hills that guides the waves to the evaluation point, and thus generate amplification.
- A checkered pattern of both hills and valleys with a fine defined pattern is the best performing checkered pattern. Vibration reduction of more than 20 % was obtained at, and nearby, the main evaluation point.

7. FURTHER WORK

The horizontal amplitudes may also be considered to make more general conclusions regarding the use of a shaped landscape in the sense of vibration reduction for traffic-loads or other external loads.

The geometrical and mechanical constraints regarding the shaped landscape, given within the MAX IV project, have been considered. In a more general study, those constraints could be neglected to generate results and conclusions that are more applicable to other projects, i.e. the parametric studies could be extended to include more parameters. Different types of loading could also be considered, e.g. simulating the traffic load as a moving transient load. Use of materials with more defined material properties in the hills, could possibly be of significant importance.

The shape of the three-dimensional architectural landscape design suggested at the MAX IV site could be investigated by means of the finite element method with dynamic analysis. The conclusions drawn in this paper may be used to improve the performance of that architectural design.

Acknowledgments

The Silent Spaces project, a part of the EU program Interreg IVA, is gratefully acknowledged for the financial support.

8. REFERENCES

[1] Andersen L., DCE Lecture No.3: Linear elastodynamic analysis, Aalborg University, 2006.

[2] Bathe K-J., Finite element procedures, Prentice Hall, New York, 2006.

[3] Chopra A. K., Dynamics of structures, Prentice Hall, Upper Saddle River, 1995.

[4] Craig Jr R. R., Structural dynamics, John Wiley & Sons, New York, 1981.

[5] Das B. M., Ramana G. V., Principles of soil dynamics, Cengage Learning, Stamford, 2011.

[6] Lee V. W., Wu X., "Application of the weighted residual method to diffraction by 2-D canyons of arbitrary shape: I. Incident SH waves", *Soil Dynamics and Earthquake Engineering*, 13, 355-364, 1994.

[7] Lee V. W., Wu X., "Application of the weighted residual method to diffraction by 2-D canyons of arbitrary shape: II. Incident P, SV and Rayleigh waves", *Soil Dynamics and Earthquake Engineering*, 13, 365-375, 1994.

[8] Mossessian T. K., Dravinski M., "Scattering of elastic waves by three-dimensional surface topographies", *Wave motion,* 11, 579-592, 1989.

[9] Norwegian Geotechnical Institute, Indata till beräkningarna för Linac-tunneln, Start-byggnaden och SPF, Report 20110012-00-3-TN, 2011.

[10] Persson P., Analysis of Vibrations in High-Tech Facility, Report TVSM-5164, Division of Structural Mechanics, Lund University, 2010.

[11] Persson P., Persson K., Analysis of Dynamic Soil-Structure Interaction at High-Tech Facility, Proceedings of NSCM-23: the 23rd Nordic Seminar on Computational Mechanics, Stockholm, 2010.

[12] Persson P., Persson K., Sandberg G., Reduction of traffic-induced vibrations at high-tech facility using trenches, Proceedings of NSCM-24: the 24rd Nordic Seminar on Computational Mechanics, Helsinki, 2011.

[13] Reinoso E., Wrobel L. C., Power H., "Three-dimensional scattering of seismic waves from topographical structures", *Soil Dynamics and Earthquake Engineering*, 16, 41-61, 2005.

[14] Richart F. E., Hall Jr. J. R., Woods R. D., Vibrations of soils and foundations, Prentice Hall, Englewood Cliffs, 1970.

[15] Sánchez-Sesma F. J., Campillo M., "Topographic effects for incident P, SV and Rayleigh waves", *Tectonophysics*, 218, 113-125, 1993.

[16] Zhou H., Chen X-F., "A study on the effect of depressed topography on Rayleigh surface wave", *Chinese journal of geophysics*, 50(4), 1018-1025, 2007.

[17] Zienkiewicz O. C., Taylor R. L., The finite element method, volume 1 and 2, MacGraw-Hill, London, 1994.